Article

One-Electron Reduction Potential for Oxygen- and Sulfur-Centered Organic Radicals in Protic and Aprotic Solvents

Marcel Schmidt am Busch, and Ernst-Walter Knapp

J. Am. Chem. Soc., **2005**, 127 (45), 15730-15737• DOI: 10.1021/ja0526923 • Publication Date (Web): 25 October 2005

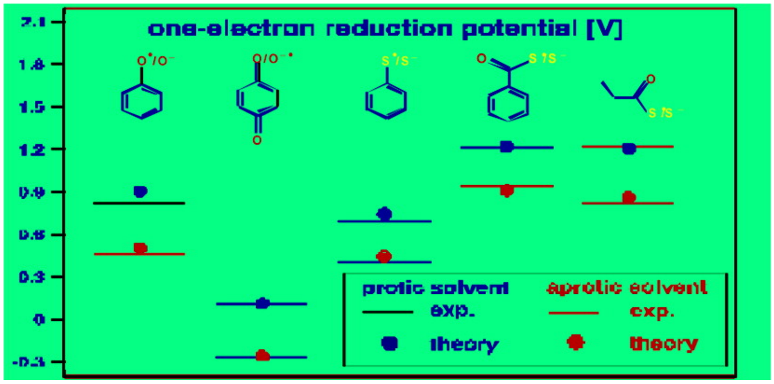

Journal of the American Chemical Society is published by the American Chemical Society. 1155 Sixteenth Street N.W., Washington, DC 20036

J|A|C|S
ARTICLES
Published on Web 10/25/2005

One-Electron Reduction Potential for Oxygen- and Sulfur-Centered Organic Radicals in Protic and Aprotic Solvents

Marcel Schmidt am Busch and Ernst-Walter Knapp*

Contribution from the Department of Biology, Chemistry, and Pharmacy, Institute of Chemistry and Biochemistry, Free University of Berlin, Takustrasse 6, 14195 Berlin, Germany

Received April 26, 2005; E-mail: knapp@chemie.fu-berlin.de

Abstract: We estimated one-electron reduction potentials of redox-active organic molecules for a spectrum of eight different functional groups (phenoxyl, *p*-benzoquinone, phenylthiyl, *p*-benzodithiyl, carboxyl, benzoyloxyl, carbthiyl, and benzoylthiyl) in protic (water) and aprotic (acetonitrile, *N*,*N*-dimethylacetamide) solvents. Electron affinities (EA) were evaluated in a vacuum with high level quantum chemical methods using Gaussian3-MP2 (G3MP2) and Becke 3 Lee, Yang, and Parr functional B3LYP with aug-cc-pVTZ basis set. To evaluate one-electron redox potentials, gas-phase free energies were combined with solvation energies obtained in a two-step computational approach. First, atomic partial charges were determined in a vacuum by the quantum chemical method B3LYP/6-31G(d,p). Second, solvation energies were determined, solving the Poisson equation with these atomic partial charges. Redox potentials computed this way, compared to experimental data for the 21 considered organic compounds in different solvents, yielded overall root-mean-square deviations of 0.058 and 0.131 V using G3MP2 or B3LYP to compute electronic energies, respectively, while B3LYP/6-31G(d,p) was used to compute solvation energies.

Introduction

A fundamental quantity to describe the redox behavior of a molecule is the standard redox potential, E°_{redox}.[1,2] The present work provides an *ab initio* computational procedure, which is transferable to evaluate redox potentials for a large spectrum of different redox-active compounds. Its feasibility is demonstrated in an application where 42 one-electron redox potentials E°_{redox} are computed for 21 redox-active organic compounds (see Figure 1) in water, a protic solvent, as well as acetonitrile (AcN) and *N*,*N*-dimethylacetamide (DMAc), which are both aprotic solvents. The 21 molecules considered in this study cover eight different functional groups, involving the radicals of phenoxyl, *p*-benzoquinone, phenylthiyl, *p*-benzodithiyl, benzoyloxyl, carboxyl, benzoylthiyl, and carbthiyl. These redox-active compounds play important roles in biochemistry, photochemistry, as well as in organic, polymer, and environmental chemistry.[3−10] All redox-active substances refer to single electron-transfer equilibria between a neutral and anionic charge state. Except for *p*-benzoquinone and *p*-benzodithiyl, which are radicals in the anionic charge state, all redox-active substances are radicals in the neutral charge state.

From the 42 computed E°_{redox} values, only 27 could be compared with available measured data in the three considered solvents.[4,5,10−20] The incompleteness of experimental redox potentials is due to limitations that refer to solvent-phase characteristics of the oxygen- and sulfur-centered radicals, which tend to be chemically unstable in the radical state.[4,5,11,12,17,21,22] The incompleteness of experimental E°_{redox} values becomes evident from Table 1, which reveals that 15 one-electron reduction potentials were measured in water[4,5,11−18] and only 12 out of 21 possible values were measured in the aprotic solvents AcN[10,19,20] or DMAc.[23] Hence, a reliable and transferable procedure to predict E°_{redox} values of redox-active com-

---

(1) Crystal, J.; Friesner, R. A. *J. Phys. Chem. A* **2000**, *104*, 2362−2366.
(2) Baik, M.-H.; Friesner, R. A. *J. Phys. Chem. A* **2002**, *106*, 7407−7412.
(3) Bauer, W.; Khüren, K. *Methoden der Organischen Chemie*, 5th ed.; Thieme Publishers: Stuttgart, Germany, 1985; pp 832−890.
(4) Harriman, A. *J. Phys. Chem.* **1987**, *91*, 6102−6104.
(5) Li, C.; Hoffman, M. Z. *J. Phys. Chem. B* **1999**, *103*, 6653−6656.
(6) Saby, C.; Luong, J. H. T. *Electroanalysis* **1997**, *10*, 7−11.
(7) Rabenstein, B.; Ullmann, G. M.; Knapp, E. W. *Biochemistry* **1998**, *37*, 2488−2495.
(8) Rabenstein, B.; Ullmann, G. M.; Knapp, E. W. *Biochemistry* **2000**, *39*, 10487−10496.
(9) Zhu, Z.; Gunner, M. R. *Biochemistry* **2005**, *44*, 82−96.
(10) Hapiot, P.; Neta, P.; Pinson, J.; Rolando, C.; Schneider, S. *New J. Chem.* **1993**, *17*, 211−224.
(11) Lind, J.; Shen, X.; Eriksen, T. E.; Merenyi, G. *J. Am. Chem. Soc.* **1990**, *112*, 479−482.
(12) Steenken, S.; Neta, P. *J. Phys. Chem.* **1982**, *86*, 3661−3667.
(13) Armstrong, D. A.; Sun, Q.; Schuler, R. H. *J. Phys. Chem.* **1996**, *100*, 9892−9899.
(14) Meisel, D.; Fessenden, R. W. *J. Am. Chem. Soc.* **1976**, *98*, 7505−7510.
(15) Wardman, P. *J. Phys. Chem. Ref. Data* **1989**, *18*, 1637−1711.
(16) Zhao, R.; Lind, J.; Merenyi, G.; Jonsson, M.; Eriksen, T. E. *J. Phys. Chem.* **2000**, *104*, 8524−8526.
(17) Zhao, R.; Lind, J.; Merenyi, G.; Eriksen, T. E. *J. Am. Chem. Soc.* **1998**, *120*, 2811−2816.
(18) Zhao, R.; Lind, J.; Merenyi, G.; Eriksen, T. E. *J. Phys. Chem.* **1999**, *103*, 71−74.
(19) Larsen, G. A.; Holm, H. A.; Roberson, M.; Daasbjerg, K. *J. Am. Chem. Soc.* **2001**, *123*, 1723−1729.
(20) Peover, M. E. *J. Chem. Soc.* **1962**, 4540−4549.
(21) Leffler, J. E. *An Introduction to Free Radicals*; John Wiley & Sons: New York, 1993; p 123.
(22) Fossey, J.; Lefort, D.; Sorba, J. Free Radicals in Organic Chemistry; Masson: Paris, 1995; p 109.
(23) Robert, J.; Anouti, M.; Paris, J. *J. Chem. Soc., Perkin Trans. 2* **1997**, 473−478.

10.1021/ja0526923 CCC: $30.25

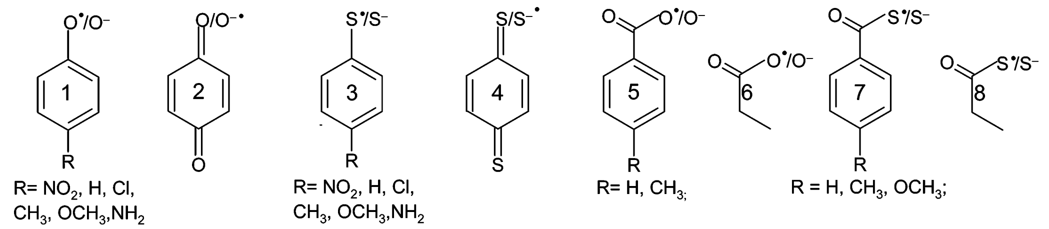

Figure 1. Redox-active compounds considered in the present work. Bold numbers label the functional groups of the redox-active compounds, which are: 1 = phenoxyl radical, 2 = *p*-benzoquinone, 3 = phenthiyl radical, 4 = *p*-benzodithiyl, 5 = benzoyloxyl radical, 6 = carboxyl radical, 7 = benzoylthiyl radical, and 8 = carbthiyl radical.

Table 1. Comparison of Directly Measured and Calculated Redox Potentials $E^{\circ}_{\mathrm{redox}}$ for the Functional Groups Depicted in Figure 1 Using the QC Method G3MP2 and B3LYP as Explained in Text[q]

		$E^{\circ}_{\mathrm{redox}}$ (V) in water			$E^{\circ}_{\mathrm{redox}}$ (V) in ACN/DMAc		
substances	formula	measured	G3MP2	B3LYP	measured	G3MP2	B3LYP
Phenoxyl Radical							
p-nitrophenoxyl radical	$\mathrm{4\text{-}NO_2{-}Ph{-}O^{\bullet}/O^{-}}$	1.28[a]/1.23[b]	1.330	1.330	0.981[k]	1.018	1.000
phenoxyl radical	$\mathrm{4\text{-}H{-}Ph{-}O^{\bullet}/O^{-}}$	0.86[a]/0.79[b]	0.906	0.758	0.461[k]	0.503	0.334
p-chlorophenoxyl radical	$\mathrm{4\text{-}Cl{-}Ph{-}O^{\bullet}/O^{-}}$	0.85[a]/0.80[b]	0.885	0.687		0.522	0.327
p-methylphenoxyl radical	$\mathrm{4\text{-}CH_3{-}Ph{-}O^{\bullet}/O^{-}}$	0.71[a]/0.68[b]	0.683	0.480	0.279[k]	0.305	0.105
p-methoxyphenoxyl radical	$\mathrm{4\text{-}CHO_3{-}Ph{-}O^{\bullet}/O^{-}}$	0.58[a]/0.54[b]/0.44[c]	0.460	0.305		0.060	−0.089
p-aminophenoxyl radical	$\mathrm{4\text{-}NH_2{-}Ph{-}O^{\bullet}/O^{-}}$	0.24[d]/0.217[e]	0.225	−0.059		−0.180	−0.454
***p*-Benzoquinone**							
p-benzoquinone	$\mathrm{O{=}Ph{=}O/O{=}Ph{-}O^{\bullet -}}$	0.10[f]/0.11[g]	0.110	0.372	−0.270[l]	−0.260	−0.001
Phenylthiyl Radical							
p-nitrophenylthiyl radical	$\mathrm{4\text{-}NO_2{-}Ph{-}S^{\bullet}/S^{-}}$		0.970	1.028	0.701[m]	0.735	0.792
phenylthiyl radical	$\mathrm{4\text{-}H{-}Ph{-}S^{\bullet}/S^{-}}$	0.69[e]	0.746	0.693	0.401[m]	0.444	0.398
p-chlorophenylthiyl radical	$\mathrm{4\text{-}Cl{-}Ph{-}S^{\bullet}/S^{-}}$		0.727	0.689	0.471[m]	0.460	0.415
p-methylphenylthiyl radical	$\mathrm{4\text{-}CH_3{-}Ph{-}S^{\bullet}/S^{-}}$	0.64[e]	0.582	0.587	0.311[m]	0.298	0.283
p-methoxyphenylthiyl radical	$\mathrm{4\text{-}CHO_3{-}Ph{-}S^{\bullet}/S^{-}}$	0.57[e]	0.472	0.419	0.181[m]	0.202	0.102
p-aminophenoxyl radical	$\mathrm{4\text{-}NH_2{-}Ph{-}S^{\bullet}/S^{-}}$	0.36[e]	0.450	0.300	−0.099[m]	0.094	−0.054
***p*-Benzodithiyl**							
p-benzodithiyl	$\mathrm{S{=}Ph{=}S/{-}S^{\bullet -}}$		0.454	0.862		0.201	0.648
Benzoyloxyl Radical							
benzoyloxyl radical[o]	$\mathrm{Ph{-}COO^{\bullet}/O^{-}}$		2.326	1.915		1.880	1.480
p-methylbenzoyloxyl radical	$\mathrm{CH_3{-}Ph{-}COO^{\bullet}/O^{-}}$		2.240	1.819		1.795	1.411
Carboxyl Radical							
propionic acid radical[o]	$\mathrm{C_2H_5{-}COO^{\bullet}/O^{-}}$		2.273	1.905		1.761	1.175
Benzoylthiyl Radical							
benzoylthiyl radical	$\mathrm{Ph{-}COS^{\bullet}/S^{-}}$	1.21[h]	1.220	1.196	0.940[n,p]	0.910	0.875
p-methylbenzoylthiyl radical	$\mathrm{CH_3{-}Ph{-}COS^{\bullet}/S^{-}}$	1.19[i]	1.210	1.120		0.842	0.767
p-methoxybenzoylthiyl radical	$\mathrm{CH_3O{-}Ph{-}COS^{\bullet}/S^{-}}$	1.17[i]	1.110	1.092		0.775	0.774
Carbthiyl Radical							
thiopropanoic acid radical[o]	$\mathrm{C_2H_5{-}COS^{\bullet}/S^{-}}$	1.22[j]	1.207	1.254	0.820[n,p]	0.860	0.920

[a] Reference 5. [b] Reference 11. [c] Reference 4. [d] Reference 12. [e] Reference 13. [f] Reference 14. [g] Reference 15. [h] Reference 16. [i] Reference 17. [j] Reference 18. [k] Reference 10. [l] Reference 20. [m] Reference 19. [n] Reference 23. [o] Estimates from bond dissociation energies (indirect measurement as discussed in text) yield $E^{\circ}_{\mathrm{redox}}$ values in water of 2.0 and 1.9 and 1.1 V for the radicals benzoyloxyl, carboxyl, and carbthiyl, respectively. [p] $E^{\circ}_{\mathrm{redox}}$ in DMAc. [q] $E^{\circ}_{\mathrm{redox}}$ values were computed for the protic solvent water and the aprotic solvents AcN and DMAc. The latter solvent was employed for the $E^{\circ}_{\mathrm{redox}}$ measurements of the benzoylthiyl and carbthiyl radicals. We do not discriminate between the two aprotic solvents in our computations, since they have virtually the same dielectric constant of $\epsilon = 37.5$. However, we use solute vdW radii, as discussed in the Methods section, that differ for the protic (water) and the aprotic (AcN/DMAc) solvents. Within each group of compounds, the entries are ordered from top to bottom with descending computed $E^{\circ}_{\mathrm{redox}}$ values. Experimental $E^{\circ}_{\mathrm{redox}}$ values are listed if available. $E^{\circ}_{\mathrm{redox}}$ values estimated from bond dissociation energies are listed in the footnote.

pounds in different solvents would be of general use to the chemical community.

In the present study, a thermodynamic cycle serves as scaffold connecting oxidized and reduced states of a redox-active compound in a vacuum and solvent to compute $E^{\circ}_{\mathrm{redox}}$ (see Scheme 1). In the current approach, we explored the quantum chemical (QC) Gaussian3-MP2 (G3MP2)[24] method, developed by Pople and co-workers to compute adiabatic electron affinities (EA)[25] accurately. Furthermore, it is demonstrated that for the computation of EA values and one-electron reduction potentials, the QC density functional theory (DFT) with the Becke 3 Lee, Yang, and Parr functional (B3LYP)[26−28] and aug-cc-pVTZ basis

Scheme 1. Thermodynamic Cycle Connecting Gas (g) and Solvent (solv) Phase for the Computation of Redox Potentials in Solution of the Redox-Active Group A

$$\begin{tikzcd}
\mathrm{A^{\bullet}(g)} \arrow[r, "\Delta G_{\mathrm{gas}}"] \arrow[d, "\Delta G_{\mathrm{solv}}(\mathrm{A})"'] & \mathrm{A^{-}(g)} \arrow[d, "\Delta G_{\mathrm{solv}}(\mathrm{A^{-}})"] \\
\mathrm{A^{\bullet}(solv)} \arrow[r, "\Delta G_{\mathrm{R}}"'] & \mathrm{A^{-}(solv)}
\end{tikzcd}$$

$$ {}^{1}/_{2}\,\mathrm{H_2(g)} \xrightarrow{\Delta G_{\mathrm{R}} = -\,4.43\ \mathrm{eV}} \mathrm{H^{+}(solv) + e^{-}}$$

---

(24) Curtiss, L. A.; Redfern, P. C.; Raghavachari, K.; Rassolov, V.; Pople, J. A. *J. Chem. Phys.* **1999**, *110*, 4703−4709.

(25) Rienstra-Kiracofe, J. C.; Tschumper, G. S.; Schaefer, H. F.; Nandi, S.; Ellison, G. B. *Chem. Rev.* **2002**, *102*, 231−282.

Table 2. Comparison of Directly Measured and Calculated EA Values and Solvation Energy Differences[j]

	EA (eV)			$\Delta\Delta G_{\text{solv}}$ (eV)	
substances	measured	G3MP2	B3LYP	water	ACN/DACA
Phenoxyl Radical					
4-NO$_2$−Ph−O$^{\bullet}$/O^{-}		3.453	3.425	−2.365	−2.039
4-H−Ph−O$^{\bullet}$/O^{-}*	2.25,[a] 2.30,[b] ≤2.36[c]	2.379	2.210	−2.980	−2.577
4-Cl−Ph−O$^{\bullet}$/O^{-}*	2.58[b]	2.626	2.446	−2.711	−2.347
4-CH$_3$−Ph−O$^{\bullet}$/O^{-}*	2.17[b]	2.251	2.060	−2.885	−2.507
4-CHO$_3$−Ph−O$^{\bullet}$/O^{-}		2.084	1.863	−2.843	−2.452
4-NH$_2$−Ph−O$^{\bullet}$/O^{-}		1.923	1.643	−2.749	−2.348
***p*-Benzoquinone**					
O═Ph═O/O═Ph−O$^{\bullet-}$	1.86,[d] 1.91,[e] 1.99[f]	1.917	2.178	−2.623	−2.246
Phenylthiyl Radical					
4-NO$_2$−Ph−S$^{\bullet}$/S^{-}		3.339	3.256	−2.092	−1.865
4-H−Ph−S$^{\bullet}$/S^{-}*	2.46,[g] ≤2.47[c]	2.515	2.287	−2.684	−2.382
4-Cl−Ph−S$^{\bullet}$/S^{-}		2.754	2.502	−2.428	−2.158
4-CH$_3$−Ph−S$^{\bullet}$/S^{-}		2.434	2.180	−2.601	−2.317
4-CHO$_3$−Ph−S$^{\bullet}$/S^{-}		2.326	2.050	−2.590	−2.317
4-NH$_2$−Ph−S$^{\bullet}$/S^{-}		2.241	1.870	−2.631	−2.346
***p*-Benzodithiyl**					
S═Ph═S/S═Ph-S$^{\bullet-}$		2.656	2.964	−2.221	−1.967
Benzoyloxyl Radical					
Ph−COO$^{\bullet}$/O^{-}*	3.75[b]	3.813	3.427	−2.975	−2.528
CH3−Ph−COO$^{\bullet}$/O^{-}		3.76	3.358	−2.970	−2.500
Carboxyl Radical					
C2H5−COO$^{\bullet}$/O^{-}*	3.43,[h] 3.40[i]	3.468	3.157	−3.254	−2.741
Benzoylthiyl Radical					
Ph−COS$^{\bullet}$/S^{-}		3.08	2.904	−2.601	−2.281
CH3−Ph−COS$^{\bullet}$/S^{-}		3.033	2.847	−2.588	−2.311
CH3O−Ph−COS$^{\bullet}$/S^{-}		3.008	2.799	−2.543	−2.259
Carbthiyl Radical					
C2H5−COS$^{\bullet}$/S^{-}		2.868	2.750	−2.796	−2.448

[a] Reference 72. [b] Reference 73. [c] Reference 74. [d] Reference 75. [e] Reference 76. [f] Reference 77. [g] Reference 78. [h] Reference 80. [i] Reference 79. [j] EA values were computed with G3MP2 and B3LYP. The computed solvation energies $\Delta\Delta G_{\text{solv}}$ for the considered compounds are listed in columns four ($\Delta\Delta G_{\text{solv}}$ in H_2O) and five ($\Delta\Delta G_{\text{solv}}$ in AcN or DMAc). DMAc was employed in experiments, which considered the E°_{redox} of the radicals benzoylthiyl and carbthiyl. Solvent dielectric constants, solvent radii, and solute atomic radii are used as explained in the Methods section. All energies are given in electronvolts. All experimental EA values were taken from the NIST webbook (http:webbook.nist.gov./chemistry/ion-ser.html).

set including diffuse functions for all atoms is in some cases as successful as the more CPU-intensive G3MP2 method, but fails completely for some compounds (see Tables 1 and 2). In the present work, electrostatic contributions to the solvation energy difference of the oxidized and reduced state of a redox-active compound were computed by solving the Poisson equation[29] with atomic partial charges derived by the restrained electrostatic potential method (RESP)[30,31] that is using QC wave functions based on DFT with the B3LYP functional and 6-31(d,p) basis set. An equivalent solvation protocol was recently applied to compute pK_a values accurately.[32]

To calculate one-electron reduction potentials in solution successfully by this procedure, two assumptions must hold. (i) The intramolecular (covalent) interactions do not depend on the environment (solvent or protein). (ii) The nonelectrostatic intermolecular van der Waals (vdW) interactions do not depend on the redox state. The success of recent studies, where redox-active cofactors in proteins[33−41] were considered, demonstrated that these assumptions generally hold in biological systems. Therefore, it is worthwhile to investigate its applicability also for redox-active compounds in solution.

In this study, we explored one-electron reduction potentials for 21 chemical and biological important compounds (see Figure 1), which accurately match the corresponding experimental data when available. The presented method is transferable to other redox-active compounds and can therefore also be used to predict reliably one-electron reduction potentials of other chemically or biologically relevant compounds where experimental data are not available.

Methods

General Scheme To Compute One-Electron Reduction Potentials. The redox potential E°_{redox} of a redox reaction $A + e^- \leftrightarrow A^-$ is proportional to the free energy difference[42]

$$\Delta G_{\text{redox}} = G(A^-) - G(A) - \Delta G_{\text{NHE}} = -FE^{\circ}_{\text{redox}} \qquad (1)$$

where $F = 23.06$ kcal mol^{-1} V^{-1} is the Faraday constant, $\Delta G_{\text{NHE}} =$

---

(26) Becke, A. D. *Phys. Rev.* **1988**, *38*, 3098−3100.
(27) Lee, C.; Yang, W.; Parr, R. G. *Phys. Rev. B* **1988**, *37*, 785−789.
(28) Becke, A. D. *J. Chem. Phys.* **1993**, *98*, 5648−5652.
(29) Warwicker, J.; Watson, H. C. *J. Mol. Biol.* **1982**, *157*, 671−679.
(30) Besler, B. H.; Merz, K. M.; Kollman, P. A. *J. Comput. Chem.* **1990**, *11*, 431−439.
(31) Bayly, C. I.; Cieplak, P.; Cornell, W. D.; Kollman, P. A. *J. Phys. Chem.* **1993**, *97*, 10269−10280.
(32) Schmidt am Busch, M.; Knapp, E. W. *ChemPhysChem* **2004**, *5*, 1513−1522.
(33) Demschuk, E.; Wade, R. C. *J. Phys. Chem.* **1996**, *100*, 17373−17387.
(34) Schaefer, M.; Karplus, M. *J. Phys. Chem.* **1996**, *100*, 1578−1599.
(35) Warshel, A.; Papazyan, A. *Curr. Opin. Struct. Biol.* **1998**, *8*, 211−217.
(36) Simonson, T.; Archontis, G.; Karplus, M. *J. Phys. Chem. B* **1999**, 6142−6156.
(37) Simonson, T.; Carlsson, J.; Case, D. A. *J. Am. Chem. Soc.* **2004**, *126*, 4167−4180.
(38) Popovic, D. M.; Zmiric, A.; Zaric, S. D.; Knapp, E. W. *J. Am. Chem. Soc.* **2002**, *124*, 3775−3782.
(39) Strajbl, M.; Shurki, A.; Warshel, A. *Proc. Natl. Acad. Sci. U.S.A.* **2003**, *100*, 14834−14839.
(40) Voigt, P.; Knapp, E. W. *J. Biol. Chem.* **2003**, *278*, 51993−52001.
(41) Ullmann, G. M. *J. Phys. Chem. B* **2000**, *104*, 6293−6301.

−4.43 eV is the energy required to take up an electron from the normal hydrogen electrode (NHE), and $E^{\circ}_{\mathrm{redox}}$ is the redox potential measured relative to NHE.[2,43,44] To convert redox potential values measured relative to standard calomel electrode (SCE), we added 0.241 V to obtain the corresponding value for NHE.[44] To calculate $E^{\circ}_{\mathrm{redox}}$, we applied

$$FE^{\circ}_{\mathrm{redox}} = \Delta G_{\mathrm{gas}} - \Delta\Delta G_{\mathrm{solv}} + \Delta G_{\mathrm{NHE}} \tag{2}$$

where

$$\Delta G_{\mathrm{gas}}(\mathrm{A}^-/\mathrm{A}) = \Delta G_{\mathrm{gas}}(\mathrm{A}^-) - \Delta G_{\mathrm{gas}}(\mathrm{A}) \tag{3}$$

is the gas-phase free energy and

$$\Delta\Delta G_{\mathrm{solv}}(\mathrm{A}^-/\mathrm{A}) = \Delta G_{\mathrm{solv}}(\mathrm{A}^-) - \Delta G_{\mathrm{solv}}(\mathrm{A}) \tag{4}$$

is the free energy difference of solvation between the reduced (A^-) and oxidized (A) state.

A conventional definition of EA (adiabatic EA) is in terms of zero temperature enthalpic gas-phase energies $H^{T=0\mathrm{K}}_{\mathrm{gas}}$ between the two charge states A^-/A, yielding[25,45]

$$\mathrm{EA}(\mathrm{A}^-/\mathrm{A}) = -\Delta H^{T=0\mathrm{K}}_{\mathrm{gas}}(\mathrm{A}^-/\mathrm{A}) = H^{T=0\mathrm{K}}_{\mathrm{gas}}(\mathrm{A}) - H^{T=0\mathrm{K}}_{\mathrm{gas}}(\mathrm{A}^-) \tag{5}$$

The enthalpy is composed of electronic energy E_0, zero-point vibration energy (ZPVE), and for nonvanishing temperature also of translational rotational vibrational (TRV) contributions $H^{T=298\mathrm{K}}_{\mathrm{TRV}}$ according to

$$H^{T=298\mathrm{K}}_{\mathrm{gas}} = E_0 + \mathrm{ZPVE} + H^{T=298\mathrm{K}}_{\mathrm{TRV}} \tag{6}$$

Similarly, the gas-phase free energy needed to compute the redox potential, eq 2, is given as the sum of electronic energy E_0, zero-point vibrational energy ZPVE, and the temperature-dependent TRV contributions to free energy according to

$$G^{T=298\mathrm{K}}_{\mathrm{gas}} = E_0 + G^{T=298\mathrm{K}}_{\mathrm{nonelectronic}} = E_0 + \mathrm{ZPVE} + G^{T=298\mathrm{K}}_{\mathrm{TRV}} \tag{7}$$

In agreement with other theoretical groups that evaluated one-electron reduction potentials[1,2,42,43,45−47] and pK_{a} values,[48−52] we applied a thermodynamic cycle (Scheme 1). High level QC methods were used to estimate gas-phase EA and ΔG_{gas}. Solvation energies were determined for a dielectric continuum model using a *one-step*[48−52] or a *two-step*[32,47] procedure as explained below in the section Computation of Solvation Energies. In the present work, we use the *two-step* procedure to evaluate solvation energies that was recently applied successfully to compute pK_{a} values[32] and to explore the conformational energy landscape of an imidazole heme complex in a dielectric medium for varying imidazole orientations.[47]

Quantum Chemical Calculations. All QC computations in the present work were based either on G3MP2[24] or on the B3LYP[26−28] functional. The three energy terms in eqs 6 and 7 were evaluated with the G3MP2[24] module of Gaussian03[53] for the oxidized and reduced states of all compounds presented in Figure 1. The QC ab initio method G3MP2 uses geometries from second-order perturbation theory [MP2/6-31G(d)] and zero-point vibrational energies from Hartree−Fock theory [HF/6-31G(d)] followed by a series of single-point energy calculations in second-order (MP2) and in fourth-order Møller−Plesset (MP4) with quadratic configuration interaction [QCISD(T)]. The MP2 calculations were performed with a new basis set, including core correlations, referred to as G3large. The QCISD(T) calculations were done with the 6-31G(d) basis set, while for MP4 basis set extensions were also used. Except for the MP2 calculations, all other single-point QC energy calculations were done with a frozen core approximation.[24]

We also computed adiabatic EA values for the same set of compounds using the B3LYP functional (see Table 2). These computations were based on molecular geometries optimized with B3LYP/6-31G(d,p) using Gaussian03.[53] The energy terms needed for the EA computation, eqs 5 and 6, were computed with Gaussian03.[53] These are the zero-point electronic energies E_0, calculated with B3LYP/aug-cc-pVTZ involving diffuse functions for all atoms, and the vibrational energies ZPVE and $G^{T=298\mathrm{K}}_{\mathrm{TRV}}$ calculated with B3LYP/6-31G(d,p) without diffuse functions. Assuming that the considered molecular species obey ideal gas partition function, ZPVE and $G^{T=298\mathrm{K}}_{\mathrm{TRV}}$ were evaluated with the same basis set (6-31G(d,p)) that was used for the geometry optimization.[45,54] This small basis set was sufficient to obtain accurate nonelectronic free energy differences between oxidized and reduced states, since variations of the vibrational energies with usage of larger basis sets were found to be small.[32] The nonelectronic free energy difference $\Delta G^{T=298\mathrm{K}}_{\mathrm{nonelectronic}} = G^{T=298\mathrm{K}}_{\mathrm{nonelectronic}}(\mathrm{A}^-) - G^{T=298\mathrm{K}}_{\mathrm{nonelectronic}}(\mathrm{A})$, eq 7, between reduced and oxidized compounds is needed to evaluate the corresponding $E^{\circ}_{\mathrm{redox}}$ eq 2, and the corresponding enthalpic energy terms, eq 6, are needed to compute the EA values, eq 5, respectively. These vibrational energy differences are in the range of 3 to 4 kcal/mol. To optimize agreement between computed and measured vibrational frequencies generally scaling factors are applied. The corresponding scaling factor of vibrational frequencies used with B3LYP/6-31G(d,p) is 0.96.[52,55] Since the differences of these terms are usually smaller than 4 kcal/mol, the influence of such a frequency scaling is negligible and was not performed in the present application.

Determination of Atomic Partial Charges. In the *two-step* procedure the solvation energy was computed using atomic partial charges determined from vacuum QC computations. The same procedure was used to determine atomic partial charges regardless whether the EA and optimized geometry of the redox-active compound were determined with G3MP2 or B3LYP. To determine atomic partial charges, a moderate basis set was used on purpose for the vacuum computations in Jaguar[56] to avoid artifacts in solute charge distribution, which are due to leakage of the electronic wave function in empty space (see discussion in the next section). With these wave functions, the RESP[30,31] procedure was applied to determine the solute atomic partial charges similarly as for recent pK_{a} computations of small organic molecules.[32] RESP matches the electrostatic potential (ESP)[57] derived from the solute QC wave function with the ESP generated by the atomic partial charges, while constraining the total charge of the solute to the appropriate value. In this procedure, the ESP is defined on grid points that are placed equidistantly on a system of rays emerging from each atom center outside of the vdW spheres of the solute atoms (defined by the atomic radii R_{vdW}) up to a maximum radius R_{max}. The corresponding R_{vdW} values are 1.95, 1.6, 1.7, 1.8, 1.96, and 2.07 Å; the R_{max} values are 9.0, 8.3, 8.5, 8.7, 9.0, and 9.5 Å for C, H, O, N, Cl, and S atoms, respectively. With a direct least-squares fit of the ESP to determine the atomic partial charges, the molecular dipole and

---

(42) Li, J.; Fisher, C. L.; Chen, J. L.; Bashford, D.; Noodleman, L. *Inorg. Chem.* **1997**, *35*, 4694−4702.
(43) Winget, P.; Weber, E. J.; Cramer, C. J.; Truhlar, D. G. *PhysChemChemPhys* **2000**, *2*, 1231−1239.
(44) Reiss, H.; Heller, A. *J. Phys. Chem.* **1985**, *89*, 4207−4213.
(45) Winget, P.; Cramer, C. J.; Truhlar, D. G. *Theor. Chem. Acc.* **2004**, *112*, 217−222.
(46) Fu, Y.; Liu, L.; Yu, H.-Z.; Wang, Y.-M.; Guo, Q.-X. *J. Am. Chem. Soc.* **2005**, *127*, 7227−7234.
(47) Galstyan, A. S.; Zaric, S. D.; Knapp, E.-W. *J. Biol. Inorg. Chem.* **2005**, *10*, 343−353.
(48) Topol, A. I.; Tawa, G. J.; Burt, S. K. *J. Phys. Chem. A* **1997**, *101*, 10075−10081.
(49) Liptak, M. D.; Shields, G. C. *J. Am. Chem. Soc.* **2001**, *123*, 7314−7319.
(50) Liptak, M. D.; Cross, K. C.; Seybold, P. G.; Feldgus, S.; Shields, G. C. *J. Am. Chem. Soc.* **2002**, *124*, 6421−6427.
(51) Chen, I.-J.; MacKerell, A. D., Jr. *Theor. Chem. Acc.* **2000**, *103*, 483−494.
(52) Jang, Y. H.; Sowers, L. C.; Cagin, T.; Goddard, W. A., III. *J. Phys. Chem. A* **2001**, *105*, 274−280.
(53) Frisch, M. J. et al. *Gaussian03*; Gaussian, Inc.: Pittsburgh, PA, 2003.
(54) Cramer, C. J. *Essentials of Computational Chemistry: Theory and Models*; Wiley: Chichester, 2002.
(55) Scott, A. P.; Radom, L. *J. Phys. Chem.* **1996**, *100*, 16502−16513.
(56) Jaguar 5.2; Schrödinger, Inc.: Portland, OR, 2003.
(57) Breneman, C. M.; Wiberg, K. B. *J. Comput. Chem.* **1990**, *11*, 361−373.

quadrupole moments are often not well reproduced. This is due to buried solute atoms whose charges are poorly defined by this method, since their influence on the ESP in the neighborhood of the solute molecule outside of the solute vdW volume is weak. Using the RESP procedure with a hyperbolic penalty function applied to all atoms except hydrogens with strength parameter $a = 0.001$ au yielded reasonable results.

Computation of Solvation Energies. Molecular solvation energies are generally evaluated directly by embedding the molecule in a dielectric medium, where the solute wave function is computed in the presence of a reaction field generated by the wave function in the surrounding dielectric medium. These QC computations are performed iteratively, adjusting the reaction field applied to the wave function until self-consistency is reached (i.e., the reaction field is equal to the electrostatic field that the wave function induces in the dielectric medium). The reaction field is calculated by solving the Poisson equation for the solute molecule in the dielectric medium representing the solvent. Many applications of this approach to estimate E°_{redox} values can be found in the literature.[1,2,42,43,45,48]

Alternatively, in this study we evaluated molecular solvation energies in two separate steps. First, solute atomic partial charges are determined under vacuum conditions with a QC method of moderate accuracy[30-32,47,58] by matching the ESP[30,31,57] based on the QC wave function with the ESP generated by the atomic partial charges using the RESP[30,31] procedure. Second, the electrostatic energies of solvation are evaluated from this point charge distribution without further involvement of QC methods by solving the Poisson equation. With this procedure, one can account for long-range effects of electrostatic energies more easily. We called this method *two-step* procedure[32,47] as opposed to the generally used direct method, which we consequently called *one-step* procedure.

The main difference between the present *two-step* and the *one-step* procedure is that in the former case the wave function used to determine the atomic partial charges is computed under vacuum conditions, while in the latter case the wave function is evaluated in a dielectric medium. Another more technical point is that in contrast to the *two-step* procedure, the *one-step* procedure is iterative.

It may look counterintuitive that the simpler *two-step* procedure should be superior to the elaborate *one-step* procedure in computing redox potentials, but with the *two-step* procedure the electron leakage problem can be better controlled, which is crucial for the quality of results obtained in the present study. The electron leakage effect is particularly strong for the loosely bound excess electron of an anionic molecule if placed in high dielectric medium, where as a consequence the electronic wave function is exploring empty space more excessively than under vacuum conditions. Thus, the electronic energy of the anionic molecular state is lowered considerably. In the real world, the empty space of dielectric medium is filled with molecules whose electrons repel each other by the Pauli exclusion principle, thus preventing excessive electron leakage. That is why in the present study the electronic wave function is computed purposely under vacuum conditions to avoid this electron leakage effect as also discussed in recent works.[32,47]

To evaluate the contribution of solvation to the redox potential of a redox-active compound, $\Delta\Delta G_{\text{solv}}(A^-/A)$, eq 4, we computed the electrostatic energy difference between gas phase and solution phase for both redox states by solving the Poisson equation for a continuum dielectric medium with $\epsilon = 1$ in the solute volume and $\epsilon_{\text{solv}} > 1$ and vanishing ionic strength in the solvent. Thus, contributions from dependencies in solute−solvent vdW interactions and solvent entropy on the redox state of a solute molecule were ignored. The latter refers to the hydrophobic effect, which would be particularly difficult to evaluate. However, unless there are solute redox state-dependent changes in solvent structure, which give rise to different nonelectrostatic solute−solvent interactions, the influence of these interactions cancels in the energy difference between oxidized and reduced species.

To compute the electrostatic energies for solvation, we used the atomic partial charges obtained with the Merz−Kollman RESP[30,31] procedure for molecular geometries optimized with G3MP2 or B3LYP/6-31G(d,p), respectively (see Table S7). The Poisson equations for these molecular charge distributions were solved with the program SOLVATE[59-61] from the electrostatic energy program suite macroscopic electrostatics with atomic detail (MEAD). In the present work, we estimated one-electron reduction potentials in water, AcN, and DMAc using $\epsilon_{\text{H}_2\text{O}} = 80$, $\epsilon_{\text{AcN}} = 37.5$, and $\epsilon_{\text{DMAc}} = 37.8$ to compute solvation from electrostatic energies. Note that the values of the dielectric constants for AcN and DMAc found in the "Dielectric Constant Reference Guide"[62] are virtually identical. The solute/solvent boundary was defined through a solvent probe radius of 1.4 Å for water and 2.0 Å for AcN and DMAc, although dependencies on solvent probe radii are weak and therefore not critical. Table S5 shows that $\Delta\Delta G_{\text{solv}}$ values increase by 10−30 meV if the probe radius is increased from 2.0 to 2.8 Å. A focusing procedure was used to solve the Poisson equation with an initial low-resolution grid of 101^3 points and 1.0 Å step size and a second high-resolution grid of 101^3 points and 0.25 Å step size centered at the solute molecule.

In combination with the G3MP2 QC method, a single set of vdW radii for solute atoms was sufficient to estimate the electrostatic solvation free energies in water for all considered redox-active compounds. These are the same vdW radii used previously for pK_a computations,[32] with the exception that the somehow artificial discrimination between aliphatic and nonaliphatic carbons was dropped in the present work. The solute vdW radii used for water are: 1.5, 1.9, 1.4, 1.4, 1.2, and 2.025 Å for C, Cl, O, N, H, and S, respectively. These vdW radii are smaller than the radii used for water in the reaction field modules PCM,[63,64] CPCM,[65,66] or in Jaguar's Poisson−Boltzmann continuum-solvation model.[52,56,67] CPCM, for instance, uses vdW carbon radii between 1.9 and 2.125 Å depending on the hybridization of the carbon atom to estimate solvation energies. Our vdW radii are close to the values of Richardson et al.,[68] who recommended the usage of small vdW radii according to suggestions from Bondi[69] to estimate solvation energies of organic molecules. As in the study of Richardson,[68] we also used an oxygen vdW radius of 1.4 Å, which is the Pauling radius also applied by Tunon et al.[70]

The adiabatic EA values computed with B3LYP for sulfur-centered radicals were lower by more than 200 meV than the corresponding experimental values (see Table 2). To regain agreement between measured and B3LYP computed E°_{redox} values of sulfur-centered radicals in water, the deviations in EA can be compensated by using a smaller sulfur radius of 1.80 Å for the evaluation of the solvation energies.

In AcN and DMAc redox-active compounds with G3MP2 and B3LYP geometries were solvated with the following set of vdW radii: 1.725, 2.1, 1.7, 1.7, 1.2, and 2.3 Å for C, Cl, O, N, H, and S, respectively. Except for the hydrogen atom these vdW radii for solvation were enhanced by about 15% for the aprotic solvents relative to the values used for protic solvents such as water. The rationale for the enhanced solute volume is discussed in the section Solvation Energies

---

(58) Wheeler, R. A. *J. Am. Chem. Soc.* **1994**, *116*, 11048−11051.

(59) Bashford, D.; Gerwert, K. *J. Mol. Biol.* **1992**, *33*, 473−486.

(60) Bashford, D.; Case, D. A.; Dalvit, C.; Tennant, L.; Wright, P. E. *Biochemistry* **1993**, *32*, 8045−8056.

(61) Bashford, D. *Curr. Opin. Struct. Biol.* **1991**, *1*, 175−184.

(62) Guide, D. C. R. Dielectric Constant Reference Guide. http://www.clipper-controls.com/info/dielectric_constants.html.

(63) Miertus, S.; Scrocco, E.; Tomasi, J. *J. Chem. Phys.* **1981**, *55*, 117−129.

(64) Miertus, S.; Tomasi, J. *J. Chem. Phys.* **1982**, *65*, 239−245.

(65) Cossi, M.; Barone, V.; Tomasi, J. *J. Chem. Phys.* **1997**, *107*, 3210−3221.

(66) Barone, V.; Cossi, M. *J. Phys. Chem. A* **1998**, *102*, 1995−2001.

(67) Greely, B. H.; Russo, T. V.; Mainz, D. T.; Friesner, R. A.; Langlois, J. M.; Goddard, W. A., III; Donnelly, R. E.; Ringalda, M. N. *J. Chem. Phys.* **1994**, *101*, 10075−10081.

(68) Richardson, W. H.; Peng, C.; Bashford, D.; Noodleman, L.; Case, D. A. *Int. J. Quantum Chem.* **1997**, *61*, 207−217.

(69) Bondi, A. *J. Phys. Chem.* **1964**, *68*, 441−551.

(70) Tunon, I.; Silla, E.; Pascual-Ahuir, J.-L. *J. Am. Chem. Soc.* **1993**, *115*, 2226−2230.

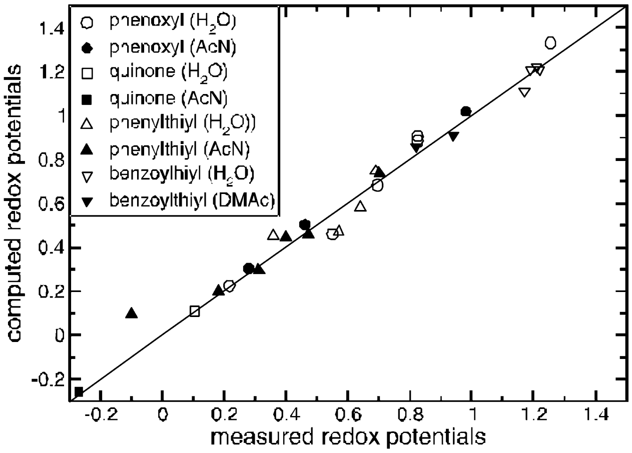

Figure 2. Correlation diagram of experimental and calculated redox potentials of the redox-active groups considered in the present work (see Figure 1). Optimized geometries and electronic and vibrational energies in the gas phase were computed with G3MP2 implemented in Gaussian03.[53] Solvation energies were calculated using atomic partial charges obtained with B3LYP/6-31G(d,p). For p-substituted phenoxyl radicals and *p*-benzoquinone, we used the average value of independent measurements (see Table 1). The RMS deviation for 27 out of 42 calculated E°_{redox} values equals 0.058 V.

in Different Solvents. Again, to obtain agreement between computed and measured E°_{redox} values for sulfur-centered radicals in aprotic solvents (AcN/DMAc), we decreased the sulfur vdW radius from 2.3 Å used for G3MP2 to 2.0 Å for B3LYP geometries (see Supporting Information, Table S2).

Results and Discussion

General Overview on E°_{redox} Computation. Experimental one-electron reduction potentials E°_{redox} often refer to the NHE, whose absolute potential is 4.43 V,[2,42,44] or to the SCE, where 0.241 V[1,2] has to be added to obtain NHE values. Figure 1 depicts eight different redox-active functional groups, which are considered in the present study and are represented by 21 compounds as listed in Table 1. For each of the considered 21 organic compounds, we computed the one-electron reduction potential, E°_{redox}, either with G3MP2 or with B3LYP in water and in AcN/DMAc and compared the values to experimental data if available (see Tables 1, S1, and S2). The overall root-mean-square (RMS) deviation between the 27 measured and computed E°_{redox} values amounts to 0.058 V for G3MP2 and 0.131V for B3LYP.[4,5,11−20,23] For B3LYP, a sulfur radius different from the one used with G3MP2 was applied to compensate for systematic errors in EA (see Methods section). From all redox-active compounds considered here, *p*-benzoquinone and *p*-benzodithiyl are the only compounds that have open-shell electronic structures in the anionic charged state. Excluding them from the considered E°_{redox} values yielded RMS deviations of 0.061 V for G3MP2 and 0.113 V for B3LYP. From the 27 experimental E°_{redox} values, 15 were measured in water[4,5,11−18] and 12 in AcN/DMAc (see Table 1).[10,19,20,23] The general agreement between computed and measured redox potentials is documented in the correlation diagram (Figure 2). If we do not consider *p*-aminophenoxyl in AcN, the overall RMS deviation for the remaining 26 experimental E°_{redox} values diminishes from 0.058 to 0.045 V for the computations with G3MP2 (see later discussion).

Experimental Error Consideration for E°_{redox}. To get an idea of uncertainties in measured redox potentials, it is instructive to consider the E°_{redox} values of substituted phenoxyls in water, which were determined by several groups.[4,5,11,12] Phenoxyl radicals rapidly dimerize in aqueous solution, yielding biphenylic compounds, which constitutes an obstacle for a reliable experimental determination of E°_{redox}. Pulse radiolysis tries to circumvent this caveat by establishing rapidly an equilibrium between the phenoxyl radical/phenolate ion couple and using a reliable redox pair as reference.[11] Except for the *p*-aminophenoxyl radical, the E°_{redox} values of all five p-substituted phenoxyl radicals considered here were measured in water by Lind et al.[11] in 1990 using pulse radiolysis. In these experiments, the error margin was between ±10 and ±20 mV except for *p*-nitrophenoxyl radical where an error of ±60 mV was given. The same five phenoxyl radicals were studied in 1999 by Li and Hoffman[5] by means of cyclic voltammetry, yielding an error of ±19 mV. Inspection of Table 1 reveals that the E°_{redox} values of the two groups deviate by 30−70 mV, which partially exceeds the internal error ranges, albeit it was considered as good agreement. Applying cyclic voltammetry, Harriman[4] obtained for the *p*-methoxyphenoxyl radical in aqueous solution $E^{\circ}_{\text{redox}} = 0.44$ V, which deviates significantly from the data of Lind et al.[11] ($E^{\circ}_{\text{redox}} = 0.54$ V) and Li and Hoffman[5] ($E^{\circ}_{\text{redox}} = 0.58$ V). These deviations are presumably due to differences in solvent composition and an associated different dimerization behavior of phenoxyl radicals. A theoretical approach possesses the formal advantage to avoid the dimerization problem explicitly.

***E°_{redox}* in Water.** The RMS deviation between computed and measured E°_{redox} values in water considering the 15 measured compounds[4,5,11−18] is 0.053 V for computations with G3MP2 (Table 1). Using B3LYP instead of G3MP2, we find that the corresponding RMS deviation is 0.145 V. Computed RMS deviations are based on averaged experimental data when available, as it is for instance for p-substituted phenoxyl radicals. Inspection of Table 1 and Figure 2 reveals that computed E°_{redox} values scatter evenly around the corresponding measured values, without systematic deviations. Since discrepancies of 30−70 mV in measured E°_{redox} values determined in different labs are considered as a good agreement,[5,11] we can confidently say that the computed one-electron reduction potentials based on G3MP2 in water displayed in Table 1 generally agree with experimental data.

Due to a lack of direct experimental data, Zhao et al.[17] estimated the E°_{redox} of the benzoyloxyl, carboxyl, and carbthiyl radicals from measured oxygen−hydrogen and sulfur−hydrogen bond dissociation energies to be 2.0, 1.9, and 1.1 V, respectively. Subsequently, they measured E°_{redox} for the carbthiyl radical directly yielding a considerably higher value of 1.21 V.[16,18] Our computed E°_{redox} for the carbthiyl radical matches with the latter experimental E°_{redox}, within 10 mV. Table 1 also reveals that the computed E°_{redox} values of the substituted benzoylthiyls,[16,18] which are the sulfur analogues of benzoyloxyl radicals, are in a good agreement with experimental data. Hence, we are confident that the computed E°_{redox} values of 2.27 and 2.32 V for the benzoyloxyl and carboxyl radical, respectively, are accurate. Considering EA values will further support the reliability of our computed one-electron reduction potentials.

***E°_{redox}* in Acetonitrile and *N,N*-Dimethylacetamide.** The E°_{redox} values of 12 of the 21 considered redox-active compounds were measured in the aprotic solvents AcN or DMAc.

The latter solvent was used to measure $E^{\circ}_{\mathrm{redox}}$ for benzoylthiyl and carbthiyl. Comparison of experimental with computed $E^{\circ}_{\mathrm{redox}}$ values based on G3MP2 yields an RMS deviation of 0.063 V. Similar to the case of water, the computed redox potentials scatter evenly around the measured values and exhibit no systematic deviation (Figure 2 and Table 1). Computed $E^{\circ}_{\mathrm{redox}}$ values based on B3LYP/aug-cc-pVTZ yielded an RMS deviation of 0.111 V (see Table 2) and are less successful.

The $E^{\circ}_{\mathrm{redox}}$ of *p*-aminophenylthiyl computed with B3LYP exceeds the measured value by 193 mV (see Table 1). Table 1 also shows that the $E^{\circ}_{\mathrm{redox}}$ values of phenylthiyl, *p*-methyl-, *p*-methoxy-, and *p*-aminophenylthiyl are downshifted, changing the solvent from water to AcN by 0.29, 0.33, 0.39, and 0.56 V, respectively. Interestingly, the solvent downshift of $E^{\circ}_{\mathrm{redox}}$ for *p*-aminophenylthiyl in AcN is much larger than that for the other three phenylthiyl radicals. On the other hand, the computed solvent downshift of $E^{\circ}_{\mathrm{redox}}$ for *p*-aminophenylthiyl changing from water to AcN is only 0.356 V and thus consistent with the other three measured solvent downshifts. If we do not consider *p*-aminophenylthiyl in the evaluation of RMS deviation for the $E^{\circ}_{\mathrm{redox}}$ values computed with G3MP2, the RMS deviation would be reduced from 0.06 to 0.03 V.

Gas-Phase Electron Affinities. Experimental EA values are available on the NIST webpage[71] for seven redox-active compounds, namely, phenoxyl,[72−74] *p*-chlorophenoxyl,[73] *p*-methylphenoxyl,[73] *p*-benzoquinone,[75−77] phenylthiyl,[74,78] benzoyloxy,[73] and carbthiyl (see Table 2).[79,80] These EA values match with the corresponding computed G3MP2 values, yielding an RMS deviation of 54 meV. The RMS deviation between measured and computed EA values based on B3LYP is 210 meV. If we neglect *p*-benzoquinone the EA values computed with G3MP2 and B3LYP match the measured values with RMS deviations of 58 and 200 meV, respectively.

The orientation of the NH_2 group of *p*-aminophenoxyl varies with the redox state in gas-phase computations performed with G3MP2. In the oxidized radical state, the amino group hydrogen atoms are in the aromatic ring plane, while in the negative nonradical state they are rotated by 90° in the out-of-plane conformation. Interestingly, computations with B3LYP favor the in-plane conformation of the amino group hydrogen atoms in both redox states. Consequently, the $E^{\circ}_{\mathrm{redox}}$ value of the *p*-aminophenoxyl radical computed in B3LYP geometry does not agree with the measured value (Table S1). Interestingly, regarding the orientation of the NH_2 group of *p*-aminophenylthiyl both QC methods favor the in-plane conformation independently of the considered redox state.

All considered redox-active compounds are radicals in the uncharged state, except for *p*-benzoquinone and *p*-benzodithiyl, which are radicals in the anionic state. Interestingly, B3LYP overestimates the EA values for *p*-benzoquinone considerably, whereas G3MP2 yields also in this case good agreement with the measured value.[75−77] Hence, we conclude that the EA value of benzodithiyl obtained with G3MP2 is reliable but not the EA value provided by B3LYP.

For some open-shell molecular species, geometry optimization may lead to different electronic states and as a consequence to slightly different geometries depending on the applied QC method. To these molecular compounds belong the charge neutral radicals of carbonic acids, which can adopt the electronic state $^2A_1$ with a symmetric pair of C−O bonds or the $^2A'$ state with unequal C−O bond lengths (broken symmetry).[81,82] For the carbonic acids benzoyloxyl and propanoyloxyl radical (Figure 1) considered in the present study, both applied QC methods (G3MP2 and B3LYP) yielded with geometry optimization broken symmetry, which means that the unpaired electron is distributed unevenly between the two oxygen atoms of the COO group. In the computation of vibrational states no imaginary frequencies were observed, which means that the true energy minima were found. The corresponding atomic coordinates are given in the Supporting Information.

Solvation Energies in Different Solvents. Solvation energies in water and the aprotic solvents AcN/DMAc were computed for the 21 considered redox-active compounds (see Figure 1) and are listed in Tables 2 and S3. These energies are based on optimized geometries in the oxidized and reduced states, which were computed with G3MP2 or B3LYP. In these computations, the solvent was modeled by a continuum dielectric medium. Experimental $E^{\circ}_{\mathrm{redox}}$ values of redox-active compounds depend on the solvent. For the 10 redox-active compounds where experimental $E^{\circ}_{\mathrm{redox}}$ values are available for both water and AcN/DMAc as solvent they are larger by 0.28−0.56 V, if solvated in water rather than in AcN/DMAc (Table 1). Surprisingly, the $E^{\circ}_{\mathrm{redox}}$ value of *p*-benzoquinone in methanol ($E^{\circ\ \mathrm{methanol}}_{\mathrm{redox}} = 100$ mV)[83] is much higher than the corresponding value in AcN ($E^{\circ}_{\mathrm{redox}} = -270$ mV, Table 1) but nearly identical to the value in water ($E^{\circ\ \mathrm{water}}_{\mathrm{redox}}$ 110 mV, Table 1). This contrasts with the values of the dielectric constant, which are close for methanol[62] and AcN[62] ($\epsilon_{\mathrm{methanol}} = 33.0$ and $\epsilon_{\mathrm{AcN}} = 37.5$), while for water it is $\epsilon_{\mathrm{H_2O}} = 80$. This puzzle is likely related to another characteristic of these solvents not related to the dielectric constant. Water and methanol have in common that they are both protic solvents and possess polar hydrogens, while AcN and DMAc are aprotic solvents, where polar hydrogens are absent. From all atoms, hydrogens possess the smallest vdW radius and can therefore come closer to solute atoms as the larger non-hydrogen atoms. This invokes large solvent−solute electrostatic interactions with polar hydrogens available in protic but not aprotic solvents. These polar hydrogens contribute significantly to solvation energies of solute molecules in protic solvents, stabilizing the anionic state and thus upshifting the redox potential. If we describe solvent molecules explicitly in atomic detail, this effect would automati-

---

(71) Bartmess, J. E. Negative Ion Energetics Data. In *NIST Chemistry WebBook*; Linstrom, P. J., Mallard, W. G., Eds.; NIST Standard Reference Database Number 69, National Institute of Standards and Technology: Gaithersburg, MD, March 2003 (http://webbook.nist.gov).

(72) Gunion, R.; Gilles, M.; Polak, M.; Lineberger, W. *Int. J. Mass Spectrom. Ion Processes* **1992**, *117*, 601−620.

(73) Fujio, M.; McIver, R. T.; Taft, R. W. *J. Am. Chem. Soc.* **1981**, *103*, 4017−4029.

(74) Richardson, J. H.; Stephenson, L. M.; Brauman, J. I. *J. Am. Chem. Soc.* **1975**, *28*, 2967−2970.

(75) Schiedt, J.; Weinkauf, R. *J. Chem. Phys.* **1999**, 304−314.

(76) Heinis, T.; Chowdbury, S.; Scott, S. L.; Kebarle, P. *J. Am. Chem. Soc.* **1988**.

(77) Marks, J.; Comita, P. B.; Brauman, J. I. *J. Am. Chem. Soc.* **1985**, *107*, 3718−3719.

(78) Taft, R. W.; Bordwell, F. G. *Acc. Chem. Res.* **1988**, *21*, 463−469.

(79) Ding, C. F.; Wang, X. B.; Wang, L. S. *J. Phys. Chem. A* **1998**, *102*, 8633−8636.

(80) Caldwell, G.; Renneboog, R.; Kebarle, P. *Can. J. Chem.* **1989**, *67*, 611−618.

(81) Rauk, A.; Armstrong, D. A. *J. Am. Chem. Soc.* **1994**, *116*, 8222−8228.

(82) Kieninger, M.; Ventura, O. N.; Suhai, A. *Int. J. Quantum Chem.* **1998**, *70*, 253−267.

(83) Jonsson, M.; Houmam, A.; Jocys, G.; Wayner, D. D. M. *J. Chem. Soc., Perkin Trans. 2* **1999**, 425−429.

cally be considered by the small vdW radius of the solvent hydrogen atoms, but in the present study solvent molecules are modeled implicitly using a single solvent radius that refers to a solvent molecule as a whole. However, varying this solvent radius cannot account appropriately for such specific effects. Hence, to consider this effect in computations of solvation energies with implicit solvent models the vdW radii of the solute atoms need to be enlarged for aprotic solvents as is done for instance in the PCM[63,64] or CPCM[65,66] methods, which are implemented in Gaussian03.[53] Enlargement of solute atom radii was also applied in the present approach.

Computations with solute atom vdW radii as used for water yielded $E^{\circ}_{\mathrm{redox}}$ values for AcN/DMAc, which are on the average only between 60 and 100 mV below the corresponding $E^{\circ}_{\mathrm{redox}}$ values for water depending also slightly on the solvent probe radius (see Table S5), while in AcN/DMAc the experimental $E^{\circ}_{\mathrm{redox}}$ values are about 300−400 mV below the corresponding values for water (Table 1). Hence, the large decrease in the dielectric constant from $\epsilon_{\mathrm{H_2O}} = 80$ to $\epsilon_{\mathrm{AcN}} = 37.5$, which diminishes in particular the stabilization of the anionic solute redox state, can account only for a fraction of the observed decrease in the experimental $E^{\circ}_{\mathrm{redox}}$ values. Thus, based on the rationale given above, we increased the vdW radii of the non-hydrogen solute atoms for the aprotic solvents AcN/DMAc by about 15% as given in the Methods section. This leads to further destabilization of the anionic solute redox state, downshifting the redox potentials correspondingly, thus yielding good agreement between computed and measured $E^{\circ}_{\mathrm{redox}}$ values as is evident form Table 1 and Figure 2.

Conclusions

In the present study, we provide a consistent procedure to compute one-electron reduction potentials for a broad spectrum of chemically important functional groups (see Figure 1) comprising oxygen- and sulfur-centered radicals in protic and aprotic solvents. The thermodynamic cycle in Scheme 1 served as a scaffold to split the energetics of the redox reaction into a gas-phase contribution and solvation-free energies. The present results revealed that QC ab initio computations based on G3MP2[24] are suitable to evaluate accurately gas-phase reaction energies (i.e., electron affinities), while less demanding QC B3LYP methods sometimes failed to provide reliable electronic energies for the open-shell anionic states.

We used a recently developed *two-step* procedure to compute electrostatic energy differences between vacuum and solvent, which was successfully applied to compute pK_a values.[32] Combining these EA and solvation energies yielded accurate redox potentials, which generally agreed with measured values within the experimental error range corresponding to an RMS deviation between a measured and computed $E^{\circ}_{\mathrm{redox}}$ value of about 50 mV. Figure 1 illustrates the general agreement between computed and experimental results. Only the computed $E^{\circ}_{\mathrm{redox}}$ value of the *p*-aminophenylthiyl radical in acetonitrile deviates considerably from the measured $E^{\circ}_{\mathrm{redox}}$ value (closed triangle in the lower left of Figure 2).

An equivalent approach was recently used to evaluate pK_a values for a large number of chemically different titratable compounds, yielding the same quality of agreement as in the present study.[32] In that approach, we could use less demanding QC DFT methods to evaluate the electronic energies, since only closed-shell electronic states were involved. We suspect that this less demanding DFT approach might also work for the computation of redox potentials of compounds involving cationic instead of anionic states. In summary, we would like to point out that with the present procedure we opened an avenue to evaluate redox potentials of medium-sized organic compounds of arbitrary composition.

Acknowledgment. This project was supported by the Deutsche Forschungsgemeinschaft SFB 498, Project A5, Forschergruppe Project KN 329/5-1/5-2, GRK 80/2, GRK 268/2, GRK 788/1. We gratefully acknowledge helpful discussions with Drs. Matthias Bickelhaupt, Richart Friesner, and Artur Galstjan. We thank Drs. Donald Bashford for providing the program MEAD.

Supporting Information Available: Complete ref 53. Tables S1 and S2 and Figures S1, S2, and S3 show one-electron reduction potentials based on B3LYP/cc-pVTZ with selective assignment of diffuse functions to atoms with unpaired electrons. Figure S4 shows computed redox-potentials in AcN/DMAc versus computed EA values for all 21 considered compounds. Figure S5 and Table S3 show the influence of the oxygen and sulfur vdW radius on $E^{\circ}_{\mathrm{redox}}$ in water. All solvation energies employed in the present study are given in Table 4a−e. All electronic E_0 and vibrational $G^{298\mathrm{K}}_{\mathrm{vib}}$ energies are provided in Table S5a−e. This material is available free of charge via the Internet at http://pubs.acs.org.

JA0526923